Science Advances
AAAS

advances.sciencemag.org/cgi/content/full/6/51/eabc5629/DC1

Supplementary Materials for

S-adenosyl-L-homocysteine hydrolase links methionine metabolism to the circadian clock and chromatin remodeling

Carolina Magdalen Greco*, Marlene Cervantes, Jean-Michel Fustin, Kakeru Ito, Nicholas Ceglia, Muntaha Samad, Jiejun Shi, Kevin Brian Koronowski, Ignasi Forne, Suman Ranjit, Jonathan Gaucher, Kenichiro Kinouchi, Rika Kojima, Enrico Gratton, Wei Li, Pierre Baldi, Axel Imhof, Hitoshi Okamura, Paolo Sassone-Corsi*

*Corresponding author. Email: psc@hs.uci.edu (P.S.-C.); grecoc@hs.uci.edu (C.M.G.)

Published 16 December 2020, *Sci. Adv.* **6**, eabc5629 (2020)
DOI: 10.1126/sciadv.abc5629

The PDF file includes:

Other Supplementary Material for this manuscript includes the following:

(available at advances.sciencemag.org/cgi/content/full/6/51/eabc5629/DC1)

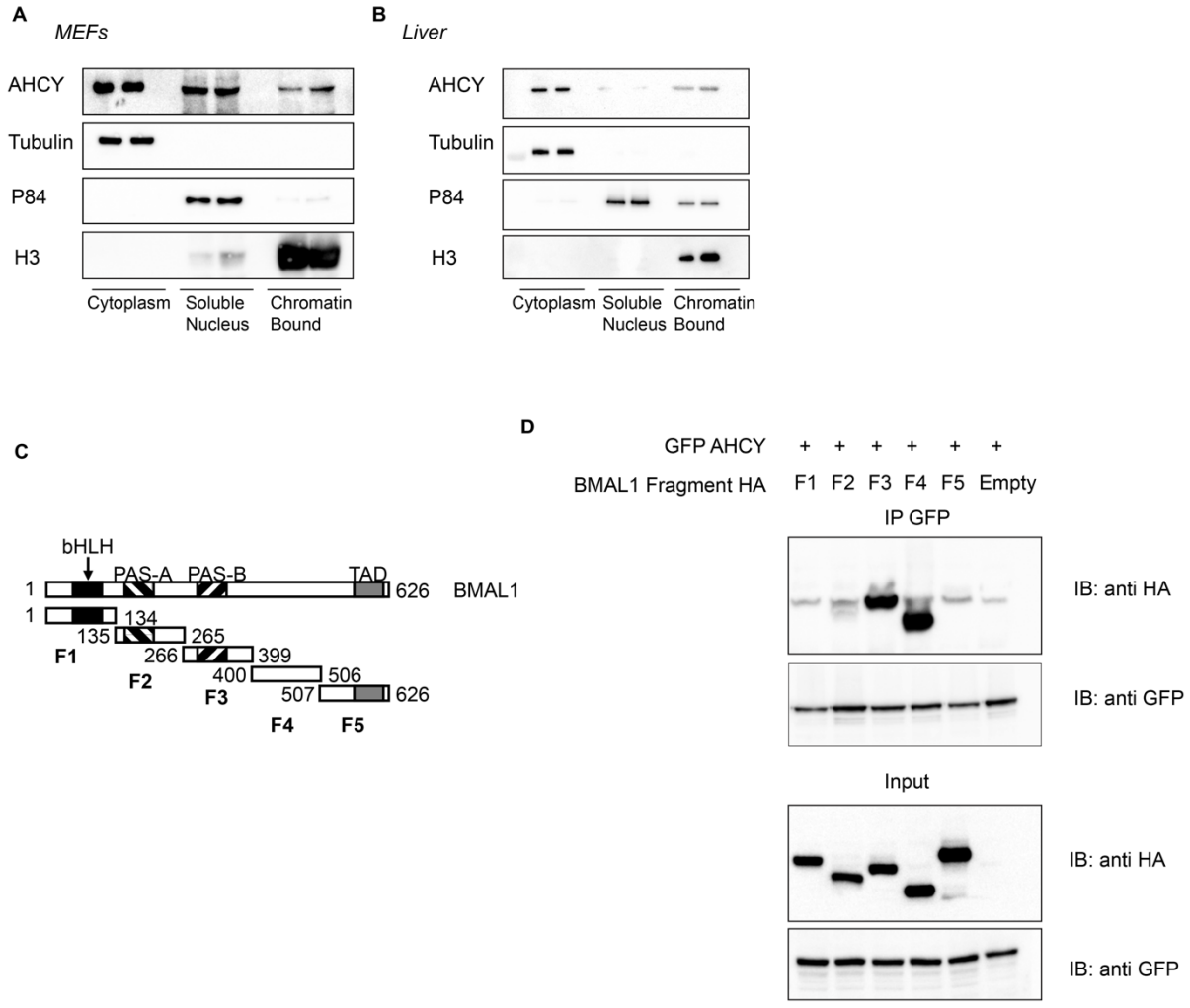

Fig. S1.

Nuclear localization of AHCY.

A, Western blot analysis of cytoplasmic, soluble nuclear and chromatin bound extracts from MEF cells for AHCY, Tubulin, P84 and histone H3. **B**, Western blot analysis of cytoplasmic, soluble nuclear and chromatin bound extracts from Liver collected at ZT8 for AHCY, Tubulin, P84 and histone H3. **C**, Schematic of GST-HA tagged BMAL1 truncations (F1-F5). **D**, Co-immunoprecipitation experiment with protein extracts from 293T cells transfected with GFP-AHCY and purified BMAL1 truncations.

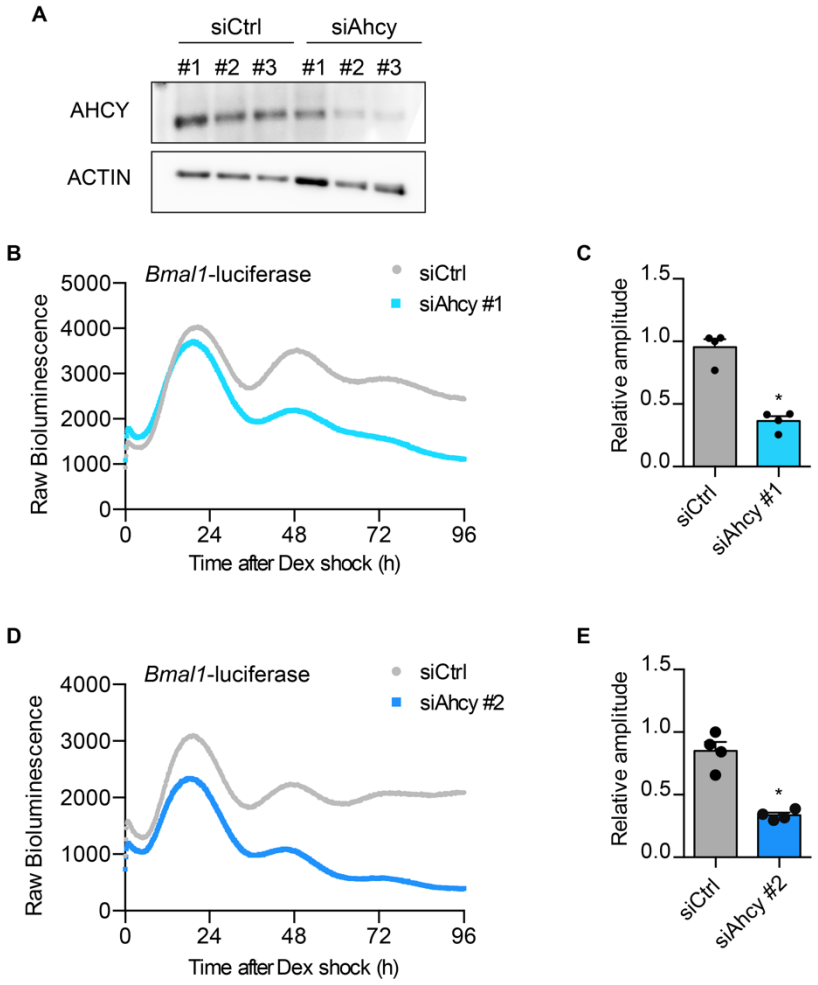

Fig. S2.

Circadian clock phenotype after knockdown of AHCY.

A, Three different siRNA were used to knockdown AHCY (siAhcy#1, siAhcy#2, siAhcy#3). Western blot result representative of four independent experiments is shown. Whole-cell lysates of siCtrl and siAhcy transfected *Bmal1:luc* U2OS cells were probed with the indicated antibodies. **B**, Bioluminescence traces for *Bmal1:luc* U2OS cells transfected either with siRNA control (siCtrl#1) or siRNA targeting Ahcy (siAhcy#1) (mean values shown, n=4). **C**, Bar graph

of relative circadian amplitude of U2OS *Bmal1:luc* siCtrl#1 and siAhcy #1 cells. (mean ± s.e.m, n=4; **P*-value ≤ 0.05; unpaired Student's t-test). **D**, Bioluminescence traces for *Bmal1:luc* U2OS cells transfected either with siRNA control (siCtrl#2) or siRNA targeting Ahcy (siAhcy#2) (mean values shown, n=4). **E**, Bar graph of relative circadian amplitude of U2OS *Bmal1:luc* siCtrl#2 and siAhcy #2 cells. (mean ± s.e.m, n=4; **P*-value ≤ 0.05; unpaired Student's t-test).

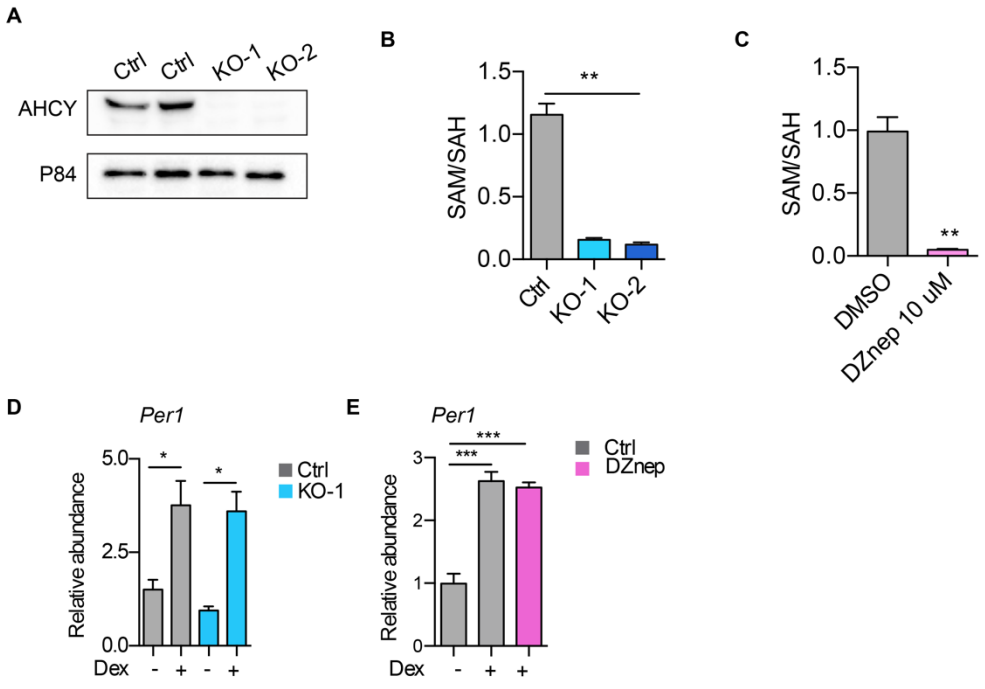

Fig. S3.

CRISPR mediated knockout and pharmacological inhibition of AHCY in MEF cells.
A, Western blot analysis showing successful knockout of AHCY by CRISPR/Cas9 in MEF cells. Whole-cell lysates were probed with the indicated antibodies. **B**, Ratio of cellular S-adenosyl homocysteine (SAH) and S-adenosyl methionine (SAM) content in control (Ctrl) and AHCY knockout (KO-1 and KO-2) MEFs (mean ± s.e.m, n=3; ***P*-value ≤ 0.01; ****P*-value ≤ 0.001; one-way ANOVA, Holm-Sidak post hoc). **C**, Ratio of cellular S-adenosyl homocysteine (SAH) and S-adenosyl methionine (SAM) content in control (DMSO) and DZnep treated MEFs (mean ± s.e.m, n=3; ***P*-value ≤ 0.01, unpaired Student's t-test). **D** Gene expression of *Per1* in (Ctrl) or AHCY null (KO-1) MEF cells 1-hour post dexamethasone treatment (mean ± s.e.m, n=3; **P*-value ≤ 0.05; unpaired Student's t-test). **E** Gene expression of *Per1* in in control (DMSO) and DZnep treated MEFs (mean ± s.e.m, n=3; ****P*-value ≤ 0.001; one-way ANOVA, Holm-Sidak post hoc).

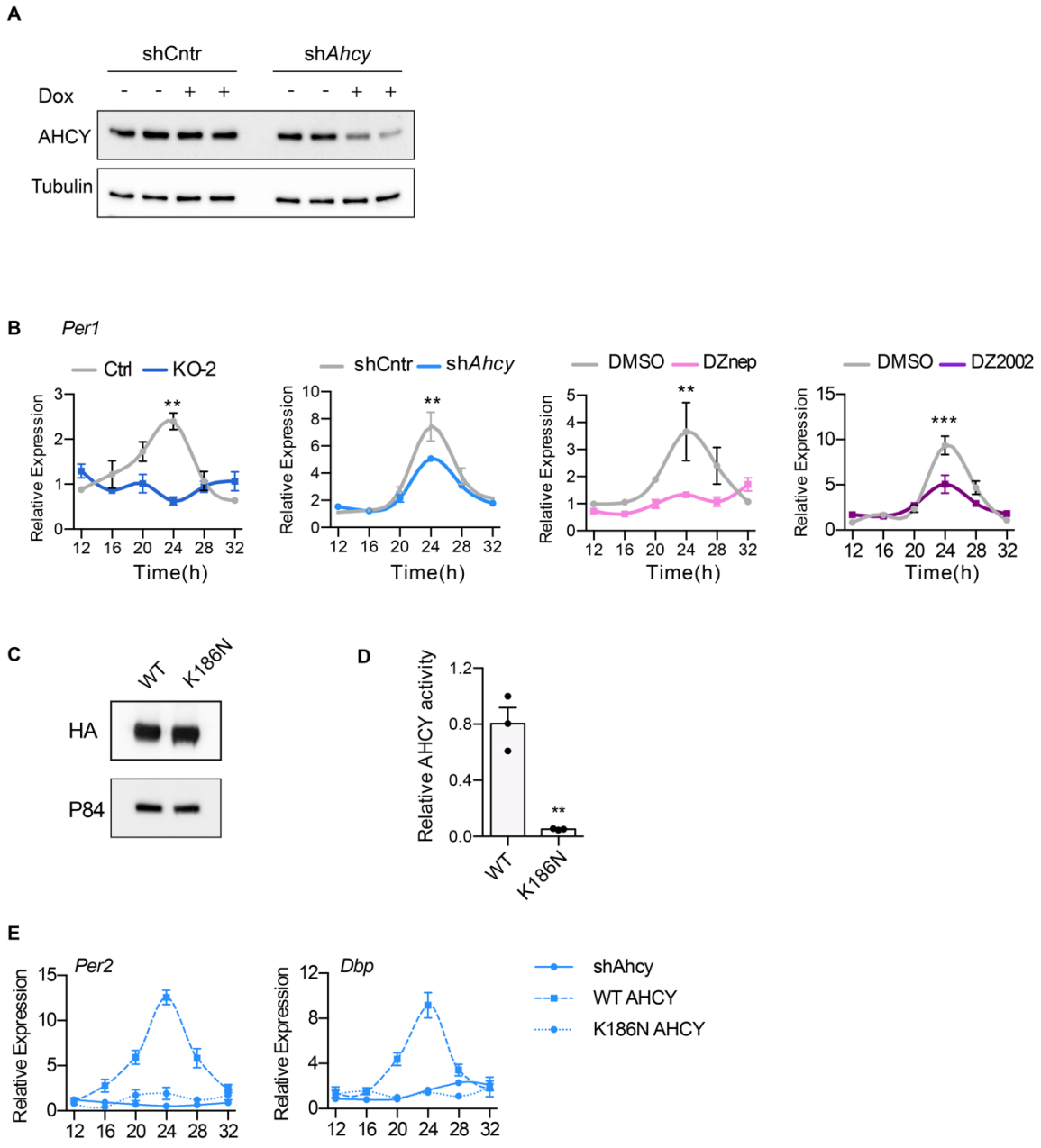

Fig. S4.

Targeting of AHCY regulates clock gene expression.

A, Western blot analysis of sh*Cntrl* and sh*Ahcy* MEF cells. Whole-cell lysates of were probed with the indicated antibodies. **B**, Circadian rhythmic expression of *Per1* in (Ctrl) or AHCY null (KO-2) MEF cells; sh*Cntrl* and sh*Ahcy* MEF cells; MEFs treated with DMSO, DeazaneplanocinA (DZnep) 10 μM and DZ2002 100 μM after dexamethasone shock (mean ± s.e.m, n=3 per time point, per group; ***P*-value ≤ 0.01; ****P*-value ≤ 0.001; ANOVA, Holm-

Sidak post hoc). **C**, Verification of MEF stable cell line. Expression levels of WT and K186N mutant HA-AHCY were verified by western blot analysis with the indicated antibodies. **D,** Measurement of WT and K186N HA-AHCY enzymatic activity from MEF stable cell lines (mean ± s.e.m, n=3; ***P*-value ≤ 0.01; unpaired Student's t-test). **E,** Circadian rhythmic expression of *Per2* and *Dbp* in cells after depletion of *Ahcy* and reconstitution of WT and K186N HA-AHCY (mean ± s.e.m, n=3 per time point, per group).

A

Correlation of Occupancy in Each 10kb Bin

BMAL1 ChIP seq

Comparison	Pearson's R
DMSO CT12 Rep1 vs Rep2	0.83
DMSO CT24 Rep1 vs Rep2	0.87
DZnep CT12 Rep1 vs Rep2	0.84
DZnep CT24 Rep1 vs Rep2	0.76

B

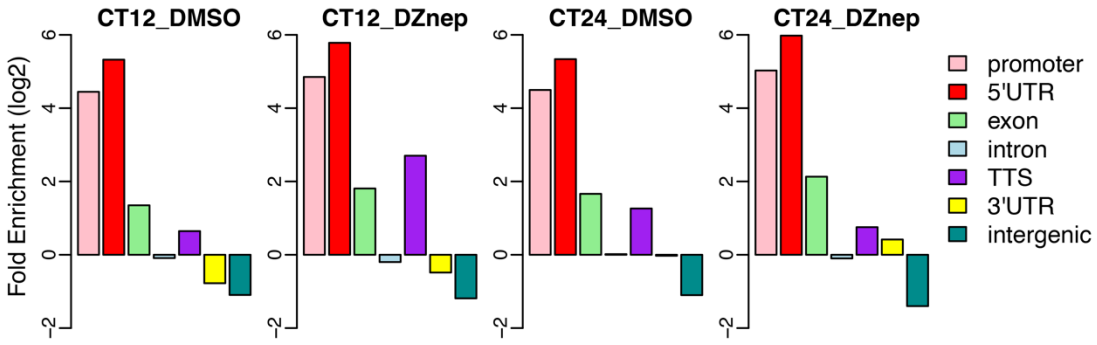

C

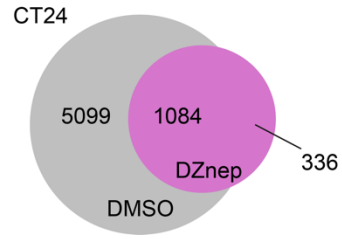

Fig. S5.

AHCY inhibition impairs rhythmic BMAL1 recruitment.

A, Table showing Pearson's correlation coefficient between biological replicates used for BMAL1 ChIP-seq. **B**, Graph of enrichment of BMAL1 peaks on different genomic elements. UTR, untranslated region; TTS, transcription termination site. **C**, Venn diagram showing the overlap of BMAL1 binding sites at CT24 between DMSO and DZnep treated MEFs.

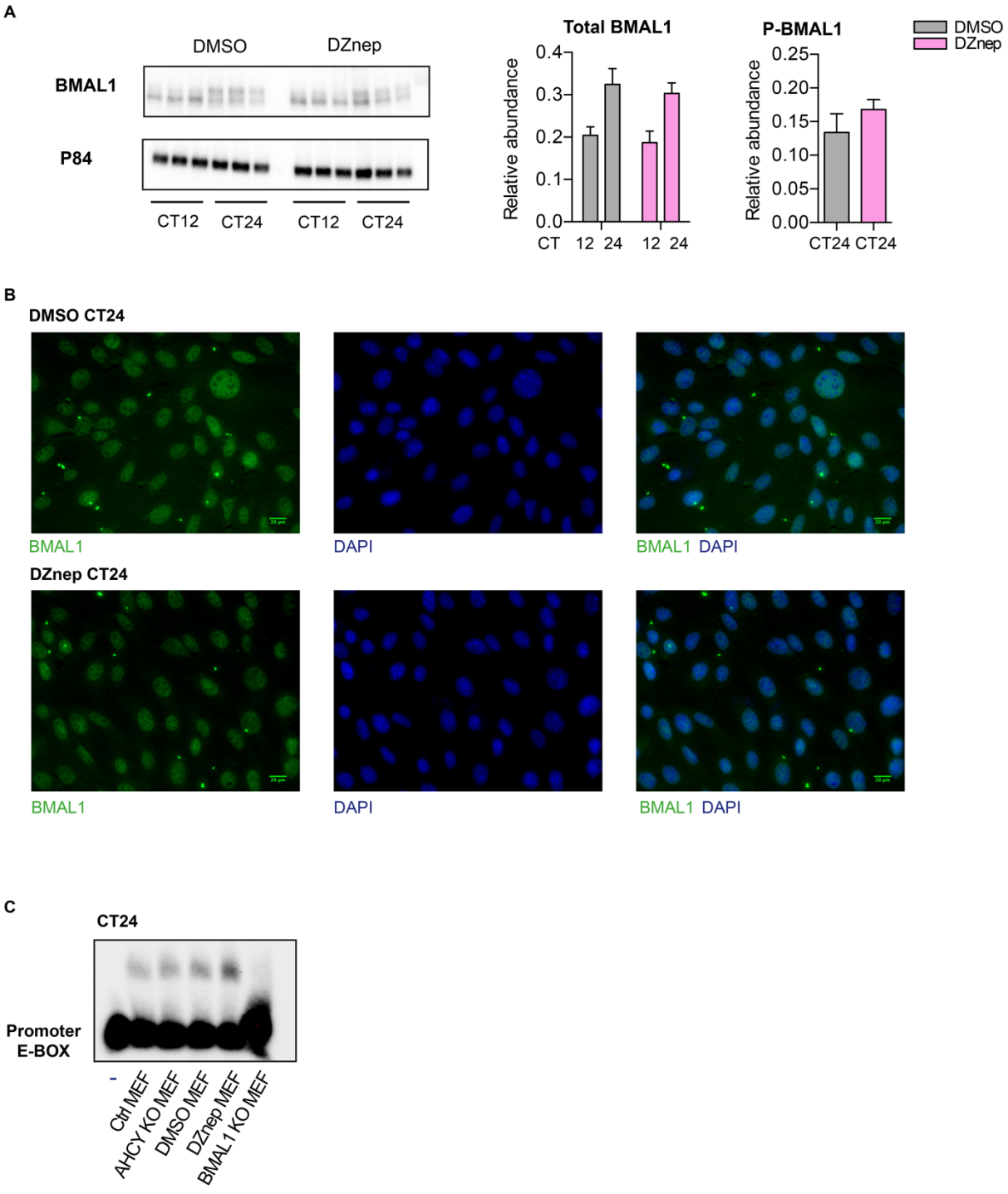

Fig. S6.

Nuclear levels and *in vitro* DNA binding of BMAL1 are unchanged upon AHCY inhibition
A, Nuclear extracts of MEF cells treated with vehicle (DMSO) or DZnep 10 μM were probed with the indicated antibodies. Quantification of total and phosphorylated BMAL1 (mean ± s.e.m,

n=3). **B**, BMAL1 was imaged by immunofluorescence microscopy in control (DMSO) and MEFs treated with DZnep 10 μM at CT24. 4',6-diamidino-2-phenylindole (DAPI) immunostaining shows nuclei. **C**, BMAL1 binding to a high affinity E-box site examined by EMSA. Nuclear extracts from the indicated cells were used.

A

H3K4me3 ChIP seq

Comparison	Pearson's R
DMSO CT12 Rep1 vs Rep2	0.98
DMSO CT24 Rep1 vs Rep2	0.98
DZnep CT12 Rep1 vs Rep2	0.98
DZnep CT24 Rep1 vs Rep2	0.97

B

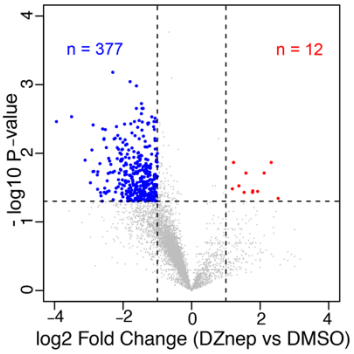

C

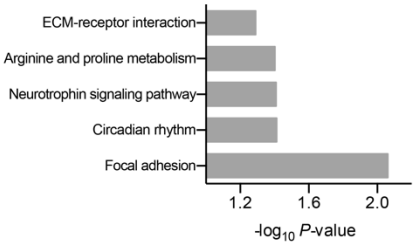

D

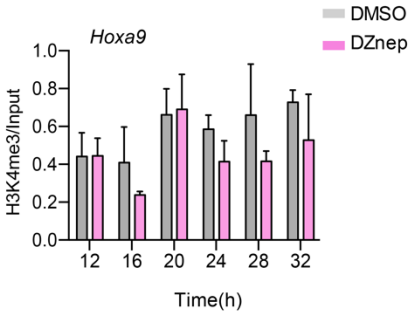

E

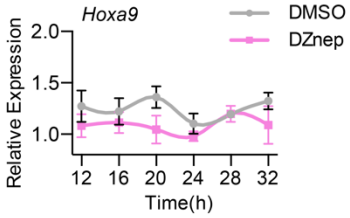

F

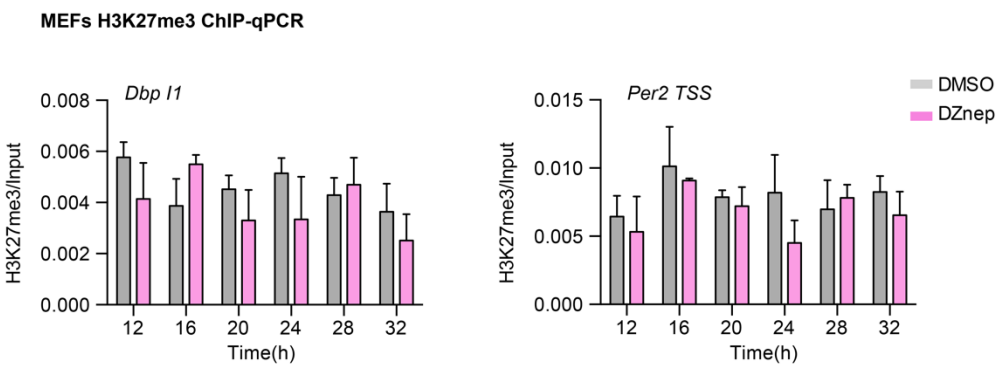

G

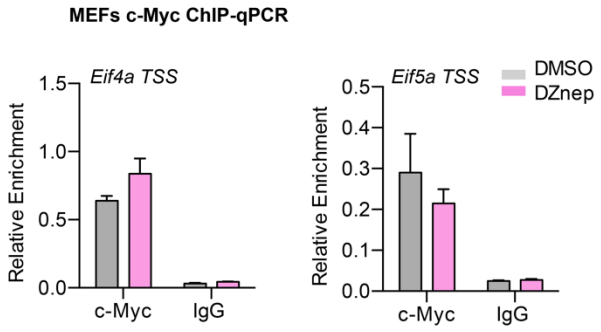

H

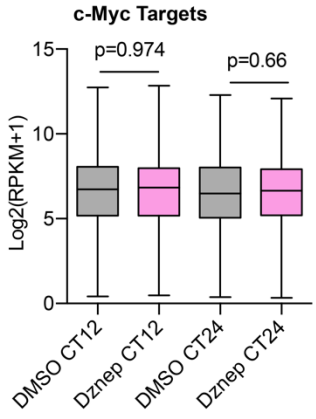

Fig. S7. AHCY inhibition impairs rhythmic H3K4me3 deposition.

A, Table showing Pearson's correlation coefficient between biological replicates used for H3K4me3 ChIP-seq. **B**, Volcano plot of genomic regions with H3K4me3 differential occupancy between vehicle (DMSO) or DZnep (10 μM) treated MEFs at CT24. **C**, GO analysis of genes associated with reduced H3K4me3 occupancy at CT24 in DZnep (10 μM) treated MEF. **D**, H3K4me3 ChIP at the *Hoxa* locus in MEFs treated with vehicle (DMSO) or DZnep (10 μM). Samples were collected at the indicated circadian times and immunoprecipitated chromatin was quantified by real-time PCR (mean ± s.e.m, n=3 per time point, per group). **E**, Expression of *Hoxa9* MEFs treated with DMSO or (DZnep) 10 μM after dexamethasone shock (mean ± s.e.m, n=3 per time point, per group). **F**, H3K27me3 ChIP at the *Dbp* and *Per2* loci in MEFs treated with vehicle (DMSO) or DZnep (10 μM). Samples were collected at the indicated circadian times and immunoprecipitated chromatin was quantified by real-time PCR (mean ± s.e.m, n=3 per time point, per group). **G**, ChIP analysis of the binding of c-Myc to target loci in MEF cells treated with DMSO or DZnep 10 μM for 24h (mean ± s.e.m, n=3). **H**, Box plot of mRNA transcript levels of c-Myc responsive genes in control (DMSO) and DZnep treated MEFs obtained from RNA-seq data.

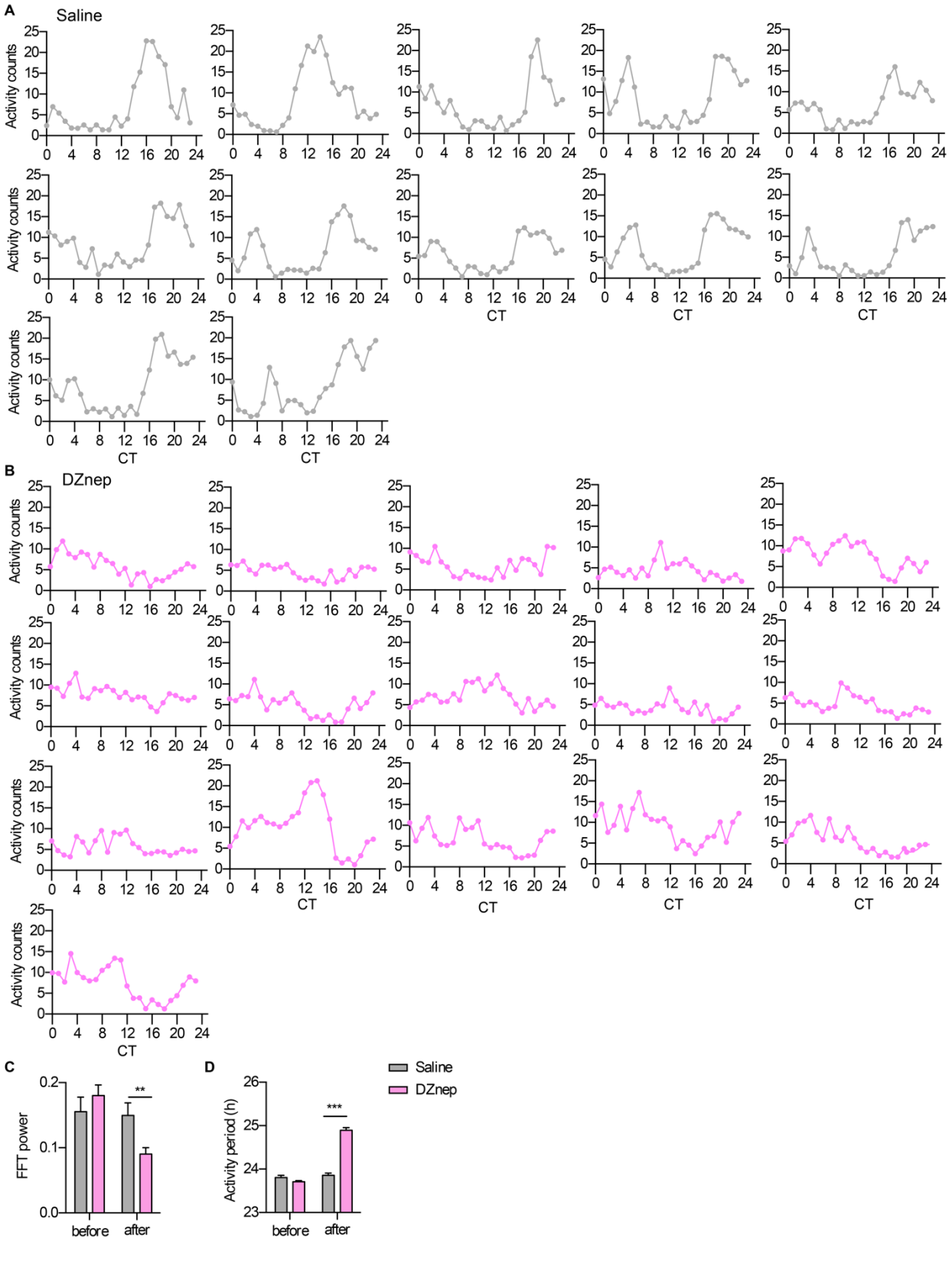
A
Saline
Activity counts
CT
B
DZnep
C
FFT power
before
after
**
D
Activity period (h)
***
Saline
DZnep

Fig. S8 Locomotor activity analysis of Saline and DZnep infused mice

A, Individual time series plots of locomotor activity from saline infused mice. **B,** Individual time series plots of locomotor activity from DZnep (100 μM) infused mice. **C,** Bar graph of amplitude of circadian rhythm represented by Fast Fourier Transform (FFT) in the circadian range in DD before and after surgery (mean ± s.e.m, n=12 Saline and n=16 DZnep; ***P*-value ≤ 0.01; ANOVA, Holm-Sidak post hoc). **D,** Bar graph of period lengths in DD before and after surgery **(**mean ± s.e.m, n=12 Saline and n=16 DZnep; ****P*-value ≤ 0.001; ANOVA, Holm-Sidak post hoc).

Fig. S9.

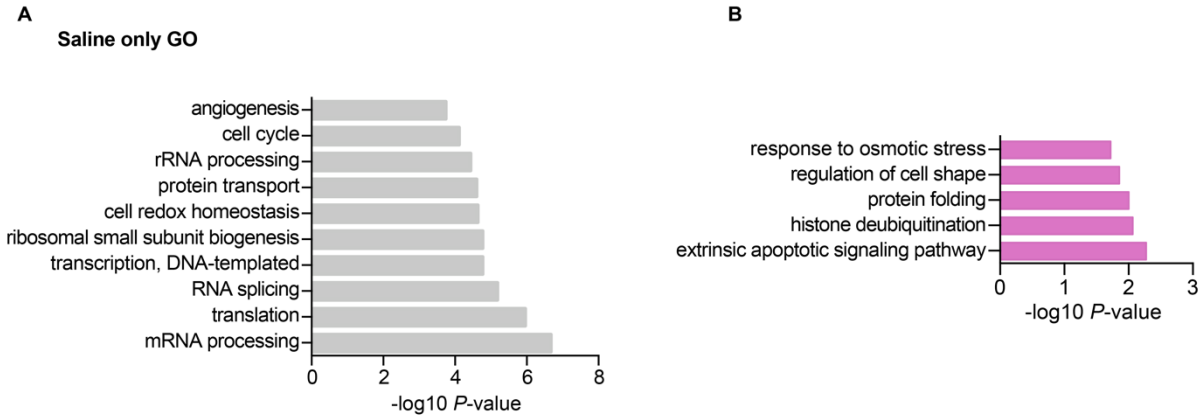

In vivo inhibition of AHCY

A, Gene ontology term enrichment analysis of genes oscillating in the saline group only. **B**, Gene ontology analysis of genes displaying higher amplitude in DZnep infused mice compared to saline.

Gene	Fw	Rev
Dbp	AATGACCTTTGAACCTGATCCCGCT	GCTCCAGTACTTCTCATCCTTCTGT
Per2	CGCCTAGAATCCCTCCTGAGA	CCACCGGCCTGTAGGATCT
Per1	ACCAGCGTGTCATGATGACATA	GTGCACAGCACCCAGTTCCC

Table S1.
Primer sequence for Real-Time qPCR (Gene expression)

Gene	Fw	Rev
Dbp I1	ATGCTCACACGGTGCAGACA	CTGCTCAGGCACATTCCTCAT
Dbp 3'UTR	GCCTGGAATGTATGAGCTAGCA	GGCACCGGAGTAGGCAAGA
Per2 TSS	AGCATCTTCATTGAGGAACCCGGG	CTCCGCTGTCACATAGTGGAAAACGTGAC
Per1 TSS	TAGTCTTTGTCCCGGAGCTT	GGAGGAGCAGAGGAGGAGAT
Nr1d1 TSS	GCCTTCAGGAGTGGCATC	CAGAAGGGTAGGACGCTGA
Hoxa9 TSS	CGCGATCCCTTTGCATAAAA	CGTAAATCACTCCGCACGCT
Eif4a	GGCACTCCGCCCTAGATT	TACTCTCGATGACGCCTTCC
Eif5a	ACCTTTCCAGAGACGCTCAC	GGGCAACATCATGATCACTTAG

Table S2.
Primer sequence for Real-Time qPCR (ChIP)

Data S1. (separate file)
LC-MS/MS analyses of BMAL1 nuclear interacting proteins.

Data S2. (separate file)
BIOCYCLE Analysis in AHCY Ctrl and KO MEF cells.

Data S3. (separate file)
Cyber-T Analysis of vehicle (DMSO) and DZnep treated MEF cells.

Data S4. (separate file)
List of genomic regions enriched for BMAL1 vehicle (DMSO) and DZnep treated MEF cells at CT12 and CT24.

Data S5. (separate file)
List of genomic regions enriched for H3K4me3 vehicle (DMSO) and DZnep treated MEF cells at CT12 and CT24.

Data S6. (separate file)
BIOCYCLE Analysis in SCN of Saline and DZnep treated mice.